Spin and orbital contributions to surface magnetism in 3d elements

Olle Eriksson, A. M. Boring, and R. C. Albers
Center for Materials Science and Theoretical Division, Los Alamos National Laboratory, Los Alamos, New Mexico 87545

G. W. Fernando
Department of Physics, University of Connecticut, Storrs, Connecticut 06268

B. R. Cooper
Center for Materials Science and Theoretical Division, Los Alamos National Laboratory, Los Alamos, New Mexico 87545
and Department of Physics, West Virginia University, Morgantown, West Virginia 26506
(Received 19 August 1991)

We have determined theoretically both the orbital and the spin contribution to the magnetic moment on the (001) surfaces of fcc Mn, bcc and fcc Fe, hcp Co, and fcc Ni. We used a surface geometry that corresponds to the bulk crystal structure (except for Mn) with no relaxation of the surface. In addition to enhanced spin moments at the surface we find that the orbital moment for surface states is greatly enhanced (sometimes by more than 100%). We also present calculations for different spin configurations in fcc Fe, and we find that two competing spin configurations exists. fcc Mn is found to have a surface spin moment slightly larger than the surface moment of bcc Fe. Detailed information from the calculations is presented, i.e., density of states, charge-density contour plots, and orbital-projected spin moments.

I. INTRODUCTION

Recent progress in theoretical and experimental techniques has contributed to a growing interest in surface physics of metals, and, more specifically, the magnetic properties of surfaces. Clean surfaces of the itinerant magnets Fe, Co, and Ni, as well as overlayers of these atoms, or their use as substrates with chemisorbed atoms, have attracted the most attention for magnetic studies. On the theoretical side, spin-polarized scalar-relativistic calculations on 3d systems have shown that the spin magnetic moment of the surface atoms is enhanced relative to the bulk atoms.[1-5] Similar effects have been found for 3d overlayers[3-8] as well as in sandwich systems.[9,10] However, all of these calculations have neglected spin-orbit relativistic effects and orbital magnetic moments, which are important in the analysis of experimental data, such as neutron scattering measurements.[11] Also relativistic effects are the dominant features of such phenomena as surface magnetic anisotropy and the magnetic-optical Kerr effect.[12]

Although most calculations are performed neglecting the spin-orbit coupling, there have been a few surface studies that do include this effect. For example, a non-self-consistent tight-binding approach[13] and a simple model calculation[14] were used to calculate the surface magnetic anisotropy of 3d elements. Self-consistent calculations of a Fe monolayer have shown the easy axis to be perpendicular to the monolayer plane, whereas for a Ni monolayer it is in the plane.[15] Subsequent calculations[16] of a free-standing Fe layer contradicted this result, finding the easy axis of magnetization to be in the plane. Although the calculations in Refs. 13–16 included the spin-orbit interaction, orbital moments were not calculated. Orbital moment results have been published[17] for Fe, Co, and Ni surfaces; these moments were obtained from a fairly simple approach, i.e., a non-self-consistent model calculation that treated the spin-orbit interaction in second-order perturbation theory.

In this paper *ab initio* spin-polarized energy-band calculations, which include spin-orbit coupling are presented, and we report on both the spin and the orbital moments for the surfaces of fcc Mn, bcc and fcc Fe, hcp Co, and fcc Ni. It has been shown that orbital moments in pure bulk materials can be significant,[18] e.g., for bulk Co. Because of the reduced symmetry and expected enhancement of the spin moment at surfaces, we anticipate an even larger orbital contribution to magnetic moments at the surface; not only for Co, but for all magnetic 3d elements.

In a previous communication[19] we reported on enhanced spin and orbital moments for the surfaces of bcc Fe, hcp Co, and fcc Ni. We have here extended our previous work to include fcc Mn and fcc Fe. The possibility of growing 3d elements epitaxially and forming structural arrangements that differ from the bulk structure makes both fcc Mn and Fe interesting. Also, for completeness, we have calculated the electronic structure of nonmagnetic Cu. The present work is a full report on our studies of surface magnetism in 3d systems, unlike the short report presented earlier.[19]

II. DETAILS OF THE CALCULATIONS

Motivated by the anticipated increased importance (relative to the bulk) of the orbital contribution to surface

magnetism, we have calculated the electronic structure by using a fully relativistic, linearized, muffin-tin-orbitals film method.[20] The technical aspects of our calculations are exactly the same as those presented in Ref. 20, and we review the most important details. A slab geometry was used; the atoms were in their bulk crystal-structure positions with no relaxation of the surface atoms. We performed the all-electron calculations with 5 to 7 atoms per unit cell, and the number of layers were increased until bulk properties (e.g., spin and orbital moments) were found for the center layer. It was found necessary to use 7 layers for all systems except hcp Co, where 5 layers already gave bulk behavior of the center layer. The basis set included 18 plane-wave orbitals[20] (PWO) together with s, p, and d muffin-tin orbitals[21] (MTO) for each atom. The warped potential was calculated according to Ref. 20; the Vosko-Wilk-Nusair parametrization[22] of the local-spin-density approximation was used. In these relativistic, self-consistent calculations the irreducible part of the two-dimensional Brillouin zone was sampled at 10–30 special k points, until the spin and orbital moments were converged. The spin-orbit coupling was included at each variational step;[21] these matrix elements can be written as

$$H_{so}=\langle \phi_{sL}\chi_s|\zeta \mathbf{L}\cdot\mathbf{S}|\phi_{s'L'}\chi_{s'}\rangle \ . \tag{1}$$

Here $\phi_{sL}\chi_s$ are the basis functions with s the spin index and L an abbreviation for the azimuthal and magnetic quantum numbers l and m_l. Furthermore $\mathbf{L}$ and $\mathbf{S}$ are the orbital and spin angular momentum, respectively, and ζ is the spin-orbit parameter. Moreover, the spin was chosen to have the quantization axis perpendicular to the surface plane and for simplicity we maintain z-reflection symmetry in the calculations. States with magnetic quantum number $\pm m_l$ will not be degenerate when Eq. (1) is added to the Hamiltonian, and we calculated the orbital moment L_z according to the Brooks and Kelly prescription:[23]

$$L_z=\sum_{\sigma,l}\sum_{m_l=-l}^{+l} n_{m_l}^{\sigma} m_l \ . \tag{2}$$

In Eq. (2) $n_{m_l}^{\sigma}$ is the number of occupied electrons for state (σ,m_l).

III. PARAMAGNETIC RESULTS

First we show our paramagnetic density of states (DOS) for fcc Mn, bcc and fcc Fe, hcp Co, fcc Ni, and fcc Cu (Fig. 1). The total DOS is here dominated by the $3d$ contribution (the shaded area). Notice that the surface bandwidths are narrower than the bulk. This is an indication that the spin moments for the surface states should be enhanced compared to the bulk. Notice also that the value of the DOS at the Fermi level (E_F) is quite high for all elements, except Cu, indicating the possibility of a

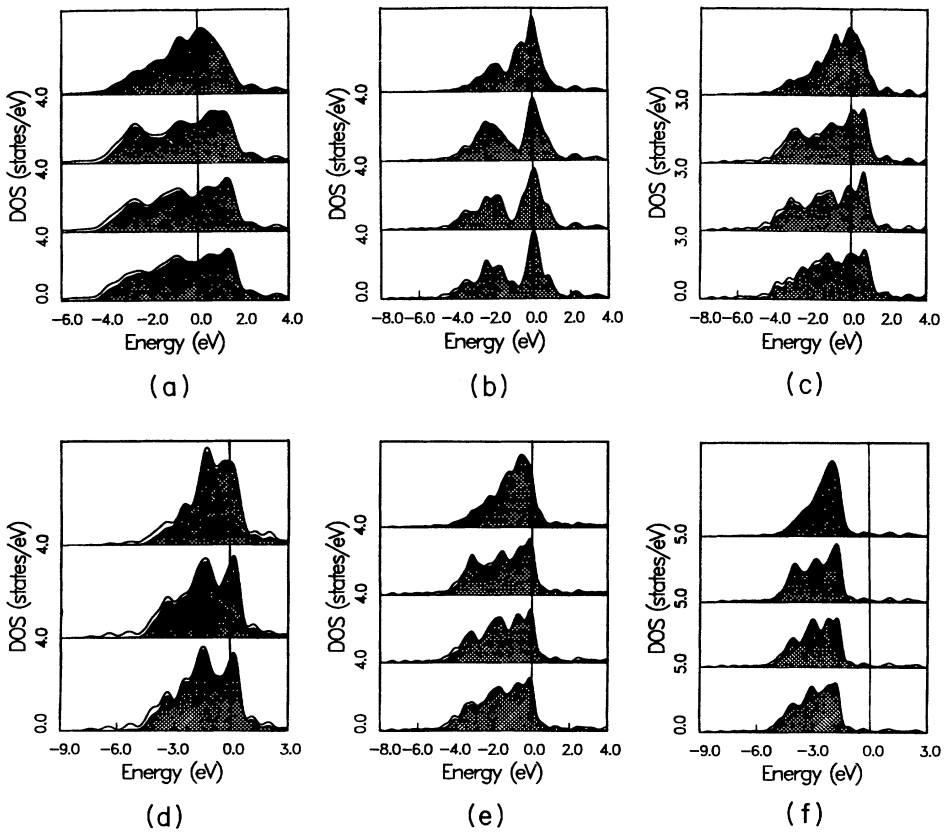

FIG. 1. Paramagnetic density of states (DOS) for fcc Mn (a), bcc Fe (b), fcc Fe (c), hcp Co (d), fcc Ni (e), and fcc Cu (f). The Fermi level is at zero and is marked with a vertical line, and units are in eV. The bulk to surface projected DOS are shown from bottom to top, respectively. The shaded area represents the $3d$ partial DOS.

Stoner product larger than one. This suggests that these systems (except Cu) will lower their total energy by becoming spin polarized. Also, the DOS becomes narrower with increasing atomic number. For instance, the bulk bandwidth of fcc Mn is approximately 6 eV whereas the bulk bandwidth of fcc Cu is about 3 eV. This is because at the end of the series more antibonding orbitals are occupied; also the $3d$ shell will experience a stronger interaction with the nucleus at the end of the series. It is also seen that the systems with the same crystal structure (fcc Mn, fcc Fe, fcc Ni, and fcc Cu) show very similar DOS, except for the above-mentioned band-narrowing effects for the heavier elements. Furthermore, the crystal-field splittings in bcc Fe into the E_g and T_{2g} components is clearly seen (Fig. 1). However, for the surface states the local geometry is far from that of the bulk, reducing this crystal field splitting. This shows up in the surface projected DOS of bcc Fe, where the decomposition in E_g and T_{2g} peaks is suppressed. This finding, as we shall see later, has implications for the orbital moments of the Fe surface.

In Fig. 2 we show the charge-density contour plots from our paramagnetic calculation. The charge density is seen to be dominated by spherical regions centered around the atomic sites. In between atoms the density is more or less flat, with a small tendency to pile up charge between the atoms. This is characteristic for metallic bonding. Notice also that the charge density in the vacuum is more or less constant parallel to the surface. Furthermore we notice that there is little difference in the charge density contours for the various crystal structures; bcc, fcc, and hcp.

The calculated paramagnetic work functions [(001) orientation for the cubic systems, and (0001) orientation for hcp Co] are 5.55, 4.53, 4.07, 5.80, 5.22, and 4.88 eV for fcc Mn, fcc Fe, bcc Fe, hcp Co, fcc Ni, and fcc Cu, respectively. Experimental data have been reported for bcc Fe [4.4–4.9 eV (Ref. 24)], hcp Co [5.0 (Ref. 25)], fcc Ni [5.2 eV (Ref. 26)], and fcc Cu [4.6–5.1 eV (Ref. 27)]. The paramagnetic work-function results are thus in good agreement with experiment, and both theory and experiment yield work functions of roughly 4–5 eV for the late $3d$ elements. As we shall see later the spin-polarized results give roughly the same work functions as the paramagnetic ones.

IV. FERROMAGNETIC RESULTS

Of the systems studied, only Cu, which has a filled d band, does not become spin polarized. Since we have done a careful study of the spin configurations of fcc Fe we will discuss the spin polarized results of fcc Fe separately, in the next section. Here we will concentrate on fcc Mn, bcc Fe, hcp Co, and fcc Ni, and we show the spin-polarized (up and down) DOS of these systems in Fig. 3. For the ferromagnetic elements, the spin polarized DOS resembles the paramagnetic DOS (Fig. 1), with an almost rigid splitting between the spin up and down DOS. As seen in Fig. 3, the surface and bulk moments are ferromagnetically ordered, except in fcc Mn where the different layers couple antiparallel [this result is similar to the bulk calculations of fcc Mn (Ref. 28)]. This antiparallel coupling in Mn leads to a spin polarized DOS of fcc Mn which is quite different from the paramagnetic DOS. An easy way to see this is to imagine the spin-up and -down bands being exchange split a large amount, so that every second layer has the spin-up band saturated, and the spin-down band above E_F (empty). For the layers in between the opposite is true (since the system is antiferromagnetic). If spin-orbit coupling is neglected the spin-up states will only hybridize and interact with other spin-up states. However if some layers have spin-up states exchange split a large amount so that they are above E_F, there will be little hybridization between occupied and empty spin-up states, and the dominating hybridization will be between every second layer (the same argument can be done for the spin-down states). This situation is different from the ferromagnetic or paramagnetic case, and it is therefore not surprising that the DOS of the paramagnetic and antiferromagnetic calculations look so different. Notice also that, with the exception of fcc Mn, the spin-up band of the surface atoms is saturated. For bulk Co and Ni the spin-up band is also saturated. This finding has implications for the relative enhancement of the surface spin moments (see below). Notice also that the crystal field splitting in both spin channels, and therefore the crystal field quenching of orbital moments, is reduced in bcc Fe in going toward the surface (just as was shown in Fig. 1). This indicates that the orbital moments of bcc Fe might be enhanced at the surface.

The calculated spin and orbital moments are given in Tables I and II. In Table I we list also the "diffuse" magnetism, i.e., the sp-projected and interstitial moments. "Diffuse" magnetism and its importance for the interpretation of experimental data has been stressed for many years. For instance, "diffuse" magnetism is believed to be the reason why the moments measured by neutron scattering experiments differ from those measured by magnetization experiments. Our results (Table I) show that the orbital moment is comparable in magnitude to the "diffuse" magnetism for bulk atoms and larger for the surface atoms (Mn is an exception, see below); this clearly demonstrates the importance of orbital moment effects on surface magnetism in $3d$ systems. Notice, also that the "diffuse magnetism" (Tables I and II) is coupled antiparallel to the total moment for all systems, except Mn. The antiferromagnetic coupling between the full moment and the sp contribution has been explained for bulk ferromagnetic Fe, Co, and Ni as an hybridization effect.[29] For antiferromagnetic systems these arguments break down and our finding of a parallel coupling between the full moment and the "diffuse magnetism" in fcc Mn might be explained by this.

The results presented in Table I show that both the surface spin and orbital moments (Mn is an exception, see below) are enhanced relative to those of the center layer (bulk moments). The enhanced spin moments are a consequence of the reduced coordination of the surface atoms, which causes narrower bands and hence larger spin moments. The orbital moment is also enhanced at the surface (sometimes by over 100%), partly due to the

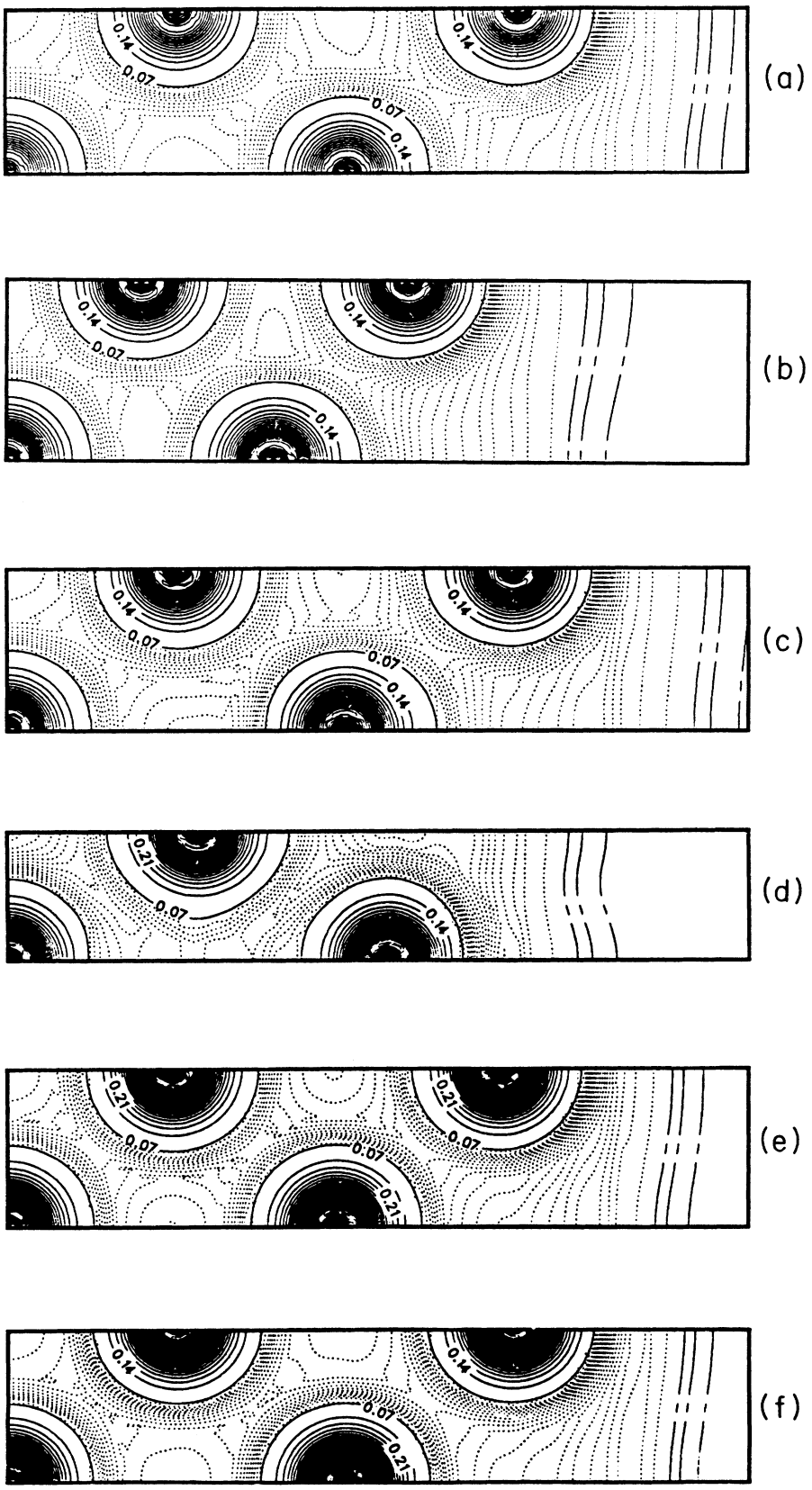

FIG. 2. Charge-density contours (in units of e^-/a.u.^{3}) obtained from the paramagnetic calculations of fcc Mn (a), bcc Fe (b), fcc Fe (c), hcp Co (d), fcc Ni (e), and fcc Cu (f). The surface is to the right in the figure, and the cut is made in the (100) plane. The spacing between solid drawn curves is 0.07, between the dotted lines 0.003, and between broken lines 0.0005.

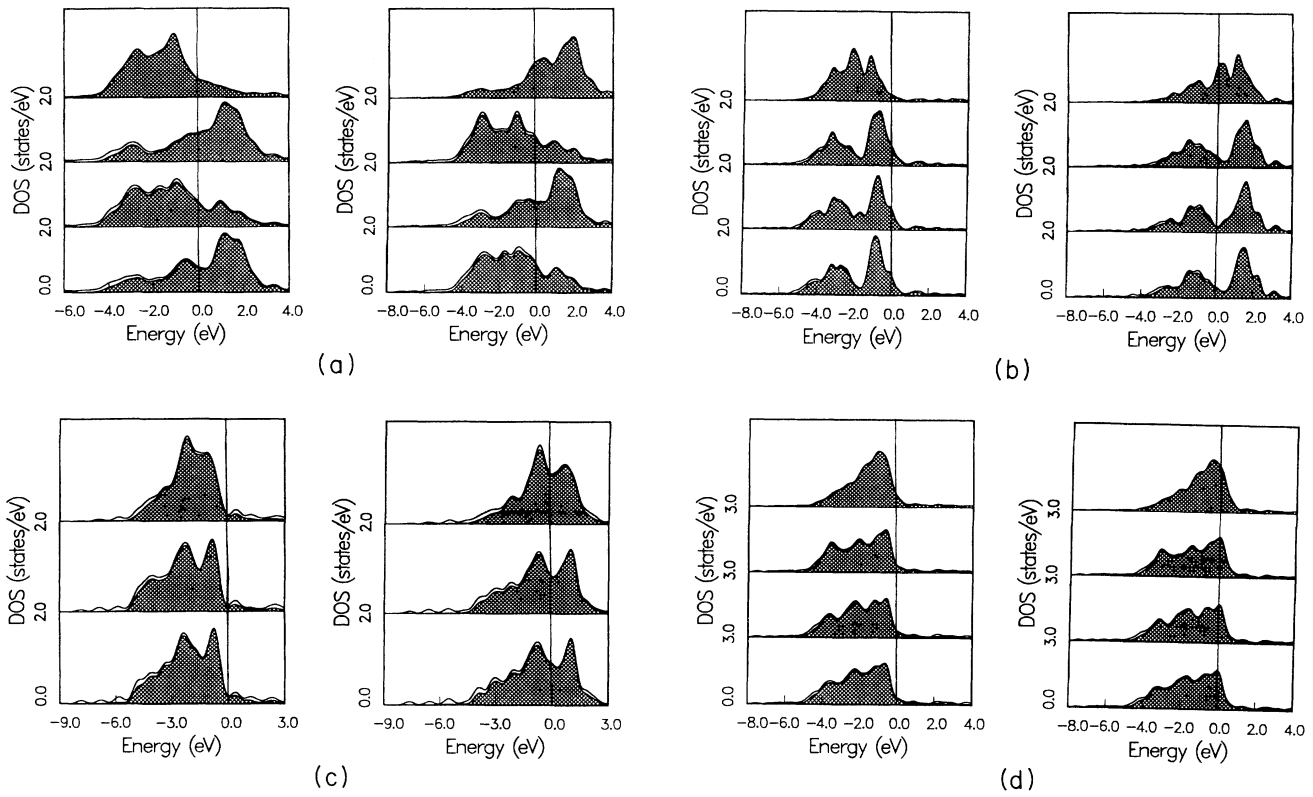

FIG. 3. Spin-polarized density of states (DOS) for fcc Mn (a), bcc Fe (b), hcp Co (c), and fcc Ni (d). The Fermi level is at zero and is marked with a vertical line, and units are in eV. The bulk to surface projected DOS are shown from bottom to top, respectively. The shaded area represents the 3*d* partial DOS. The spin-up DOS is to the left in the figure, and the spin-down DOS is to the right.

enhanced spin moment, but also due to the lower symmetry, which reduces the crystal-field quenching of the orbital moment. In addition, at the surface, the higher density of states (DOS) at the Fermi level (E_F) tends to increase the orbital moment for reasons given in Refs. 30 and 31. Almost all of the calculations, therefore, show a clear correlation between spin and orbital moments, in that enhanced surface spin moments are accompanied by enhanced surface orbital moments. However, this correlation between spin and orbital moments do not hold up well under closer scrutiny. For instance, bcc Fe has a larger center-layer spin moment than hcp Co, but a smaller center-layer orbital moment; this is in agreement with our previous investigations[30] for bulk Fe, Co, and Ni, where we found that the orbital moment is also affected by the crystalline environment and band-filling

TABLE I. Calculated total, spin, orbital, and "diffuse" moments for fcc Mn, bcc Fe, hcp Co, and fcc Ni in units of μ_B. The diffuse moment is the sum of the interstitial moment and the *sp* magnetism, per atom.

		$\mu_{\text{tot}}^{\text{spin}}$	$\mu_{\text{tot}}^{\text{orb}}$	μ_{tot}	μ_{diffuse}
	Bulk	−1.83	−0.02	−1.85	−0.01
fcc Mn	Sub-subsurface	1.86	0.02	1.88	0.08
	Subsurface	−2.11	−0.02	−2.13	−0.03
	Surface	2.89	0.02	2.91	0.09
	Bulk	2.18	0.05	2.23	−0.04
bcc Fe	Sub-subsurface	2.33	0.05	2.38	−0.04
	Subsurface	2.34	0.06	2.40	−0.04
	Surface	2.87	0.12	2.99	0.00
	Bulk	1.58	0.09	1.67	−0.07
hcp Co	Subsurface	1.67	0.09	1.76	−0.08
	Surface	1.75	0.11	1.86	−0.07
	Bulk	0.55	0.04	0.59	−0.04
fcc Ni	Sub-subsurface	0.57	0.04	0.61	−0.04
	Subsurface	0.58	0.05	0.63	−0.04
	Surface	0.59	0.06	0.65	−0.03

TABLE II. Calculated *spd* projected spin moments of fcc Mn, bcc Fe, hcp Co, and fcc Ni in units of μ_B.

		μ_s^{spin}	μ_p^{spin}	μ_d^{spin}	μ_{tot}^{spin}
	Bulk	−0.020	−0.023	−1.786	−1.829
fcc Mn	Sub-subsurface	0.022	0.031	1.805	1.858
	Subsurface	−0.026	−0.037	−2.050	−2.113
	Surface	0.030	0.032	2.828	2.890
	Bulk	−0.006	−0.020	2.205	2.179
bcc Fe	Sub-subsurface	−0.002	−0.025	2.353	2.326
	Subsurface	−0.007	−0.020	2.363	2.336
	Surface	0.009	0.008	2.851	2.868
	Bulk	−0.008	−0.035	1.625	1.582
hcp Co	Subsurface	−0.015	−0.034	1.721	1.672
	Surface	−0.008	−0.030	1.784	1.746
	Bulk	−0.005	−0.017	0.570	0.548
fcc Ni	Sub-subsurface	−0.005	−0.018	0.596	0.573
	Subsurface	−0.006	−0.017	0.598	0.575
	Surface	−0.002	−0.012	0.600	0.586

effects. The results of fcc Mn demonstrates the importance of band-filling effects quite clearly. Hund's third rule states that the spin and orbital moment should be antiparallel for systems with less than a half-filled shell, and parallel for systems with more than a half-filled shell. Mn has approximately 5 $3d$-electrons and is consequently a borderline case, which explains the tiny orbital moment (Table I). Since our calculations for fcc Mn give a $3d$ occupation slightly larger than 5, our results are in accord with Hunds rules; we find the spin and orbital moment to be parallel.

Bcc Fe has the largest orbital surface enhancement, which gives a surface orbital moment that is even slightly larger than on Co, in contrast to the comparison between bulk orbital moments. This turnabout is due to the relatively modest increase in the Co surface orbital moment; the Co surface spin moment is also not very enhanced. These effects are probably because the lowering of the symmetry at the surface of a hcp crystal is not as pronounced as in a bcc crystal, since bulk hcp already has a lower symmetry than bulk bcc. Furthermore the surface spin moment of bcc Fe is much larger than in hcp Co. Also, the enhancement of the surface DOS with respect to the bulk DOS at E_F, which tends to increase the orbital moment,[30,31] is not as large for Co as it is for Fe.

The surface spin-moment enhancements over the bulk values is 7% for fcc Ni, 10% for hcp Co, 32% for bcc Fe, and 58% for fcc Mn. The reason for the much larger increase in Mn and Fe relative to Co and Ni is that the spin-up band is saturated in bulk Co and Ni, and hence the increased spin moment at the surface is due to the reduced number of spin-down electrons. Bulk Mn and Fe do not have a saturated spin-up band; therefore, the surface states can have more spin-up as well as less spin-down electrons relative to the bulk, and these two effects cooperate to give a very large moment at the surface. The magnitude of the surface spin moment of bcc Fe ($2.87\mu_B$) is actually close to saturation. Notice in Table I that the largest surface spin moment is found for fcc Mn, despite the fact that the bulk moment of fcc Mn is smaller than for bulk bcc Fe.

The calculated work functions [(001) orientation for the cubic materials and (0001) orientation for hcp Co] are 4.58, 4.30, 5.69, and 5.02 eV for fcc Mn, bcc Fe, hcp Co, and fcc Ni, respectively. These values are quite close to the paramagnetic ones, and the agreement with experiment[24–27] is good. The largest change in work function, due to spin ordering, is found in the antiferromagnetic system, fcc Mn.

V. FCC IRON

It has been reported earlier that the interatomic exchange coupling in fcc Fe is ferromagnetic when the spin moment exceeds $2.3\mu_B$, and antiferromagnetic otherwise[28] (more studies of the various spin configurations and total energies of fcc and bcc Fe can be found in Ref. 32). In accord with this, it was found in a surface study, utilizing a 5-layer calculation of fcc Fe that the surface and subsurface layers were parallel, whereas the subsurface and center layers were antiparallel.[4] To further investigate the coupling of the spins in fcc Fe, we have here performed a 7-layer calculation (for clarity we denote the different layers as follows: surface S, subsurface S-1, sub-subsurface S-2, and center C). In Ref. 4 it was found that the surface layer had a moment larger than the "magic" moment of $2.3\mu_B$, whereas the center layer moment was lower. We expect this to be the case also for a 7-layer calculation. Hence, if the arguments above hold[28] we expect that the S and S-1 layers are ferromagnetically coupled with all other layers antiferromagnetically coupled; we represent this coupling as $++-+-++$. Much to our surprise we find that there exists two competing spin configurations. One is the expected $++-+-++$ configuration with spin moments 2.78, 2.14, −1.68, and $1.53\mu_B$ and orbital moments 0.08, 0.07, −0.06, $0.06\mu_B$, for the surface to center layer, respectively. The other spin configuration is $-+-+-+-$, and has spin moments −2.52, 1.36, −1.47, and $1.39\mu_B$ and orbital moments −0.08, 0.07, −0.05, $0.06\mu_B$ for the surface to center layer, respectively. These results are in accord with the finding of Ref. 28

since the average of the magnitude of the moment for the surface and subsurface is $2.46\mu_B$ (larger than $2.3\mu_B$) for the $++-+-++$ configuration, and $1.94\mu_B$ (smaller than $2.3\mu_B$) for the $-+-+-+-$ configuration. We also find that due to the increased sublattice moments the $++-+-++$ configuration is energetically favored. This configuration has the same spin arrangement at the surface as the 5-layer calculation.[4] It is interesting that the surface and subsurface moments in the 5- and 7-layer calculations, with equal spin configuration, are quite similar.

The calculated work functions for the two different spin configurations of fcc Fe are approximately the same; ~4.8–4.9 eV. This value differs ~0.3–0.4 eV, from the paramagnetic result. A similar, but more pronounced, effect was found for fcc Mn where the difference in work function between the paramagnetic and spin polarized state was ~1 eV. Fcc Fe and fcc Mn have in common an antiferromagnetic coupling between atoms (see also Ref. 28), which results in an electronic structure quite different from the paramagnetic or ferromagnetic ones. The antiferromagnetic coupling in fcc Fe and fcc Mn, and the accompanying change in electronic structure, is the reason for the relatively large modification of the work function due to spin ordering.

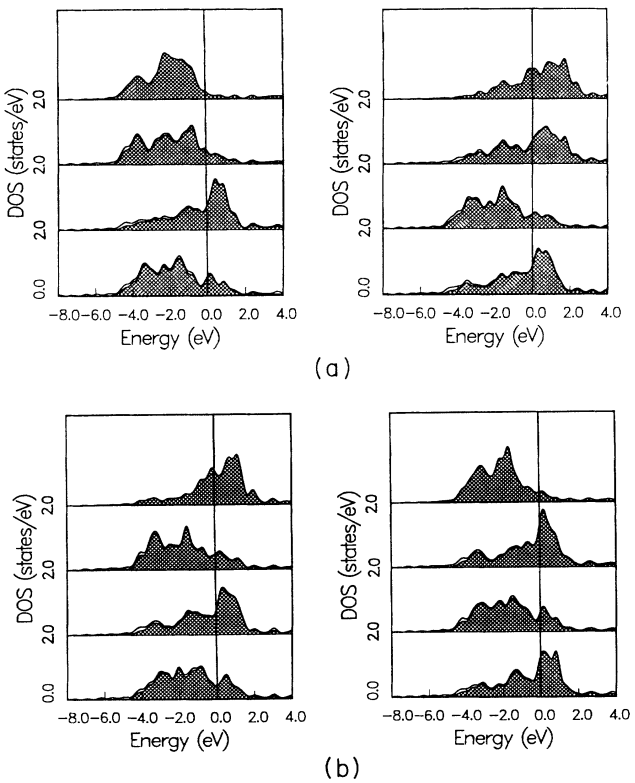

FIG. 4. Spin-polarized density of states (DOS) for the seven-layer calculation of Fe. The $++-+-++$ configuration is shown in (a) and the $-+-+-+-$ configuration is shown in (b). The Fermi level is at zero and is marked with a vertical line, and units are in eV. The bulk to surface projected DOS are shown from bottom to top, respectively. The shaded area represents the 3*d* partial DOS. The spin-up DOS is to the left in the figure, and the spin-down DOS is to the right.

The DOS for the two spin configurations are displayed in Fig. 4. Notice that the spin polarized DOS looks quite different compared to the paramagnetic one (Fig. 1) and that the spin polarized DOS of the $-+-+-+-$ spin configuration is quite similar to the spin polarized DOS of fcc Mn [Fig. 3(a)], since these two systems have the same type of spin configuration. Notice also that the bulk and $S-2$ projected DOS for the two spin configurations in Fe are very similar. These two layers have the same local spin configuration, which produces the similarity. However the rest of the layers have different local spin configurations, and correspondingly the DOS also look different.

VI. CONCLUSIONS

To conclude, we have calculated, *ab initio,* orbital as well as spin moments for a surface and shown that bcc and fcc Fe, hcp Co, and fcc Ni have a large enhancement of, not only the spin, but also the orbital moment at the surface. The enhanced orbital moment at the surface is caused by the enhanced spin moment and the lowering of the symmetry at the surface, which cooperate to yield an enhancement of the surface orbital moment sometimes as large as more than 100%. Orbital effects are important for analyzing experiments that probe surface magnetism. For instance, it is known that "diffuse" spin magnetism in these systems sometimes makes the interpretation of experimental data uncertain (e.g., when comparing moments from neutron scattering experiments with moments obtained from magnetization measurements). The present work shows that the surface orbital moment is appreciably larger than this "diffuse" magnetism in 3*d* systems (except for fcc Mn). We anticipate that the enhancement of the orbital moment will be even more pronounced in systems where relativistic effects are known to be even more important, e.g., actinide systems, where the spin-orbit parameter is larger than in the 3*d* elements and crystal-field effect is less important. It is also interesting to compare our self-consistent calculations with the non-self-consistent, perturbation calculation of Bruno.[17] The agreement is good. Since the spin-orbit splitting in the 3*d* elements is fairly small, a second-order perturbation approach, presented in Ref. 17, is a good approximation.

Furthermore, the inclusion of the spin-orbit coupling is found not to affect some ground-state properties, since our calculated spin moments (and occupation numbers) agree with previous scalar relativistic results.[1–10] Also previous published DOS, work functions, and spin density contours[1–10] (now shown here) are very similar to our results.

Moreover, the present work shows that the surface spin moment of fcc Mn is larger than in bcc Fe, whereas the orbital moment in Mn is tiny. This latter finding is in accord with Hund's third rule making Mn a borderline case where the spin and orbital coupling is about to change from antiparallel to parallel. Therefore we predict that the (001) surface of fcc Mn (if it could be stabilized by epitaxial growth) should have a large *isotropic,* spin moment. The finding of a very large spin moment in

fcc Mn is interesting. The late $3d$ elements (Cr-Ni) all show magnetic ordering, except Mn. This despite the fact that Mn has the most unpaired electrons and could in principle gain the most exchange energy due to spin polarization. On the other hand Mn can fill all bonding $3d$ states, leaving the antibonding states empty. In bulk Mn the latter effect apparently dominates and the maximized bonding in α-Mn is also associated with a very low symmetry crystal structure. By restraining Mn to have the fcc structure, the polarized solution becomes stable with a substantial spin moment.[28]

The quite complicated spin configurations of the (001) surface of fcc Fe has been carefully studied and we find that there exists two competing configurations. Both these configurations are in agreement with the finding of Ref. 28, namely, that fcc Fe has an antiferromagnetic interatomic coupling when the spin moment is smaller than $\sim 2.3\mu_B$, and a ferromagnetic coupling otherwise. This causes the interesting situation that the surface to subsurface coupling is predicted to be ferromagnetic;[4] whereas the interior (bulk) coupling is antiferromagnetic.

ACKNOWLEDGEMENTS

This work was performed under the auspices of the U.S. Department of Energy. The support from the Nuclear Material Technology Division at Los Alamos is appreciated. Valuable discussions with P. Weinberger are acknowledged.

[1]C. S. Wang and A. J. Freeman, J. Magn. Magn. Mater. **15-18**, 869 (1980); C. S. Wang and A. J. Freeman, Phys. Rev. B **24**, 4364 (1981).

[2]O. Jepsen, J. Madsen, and O. K. Andersen, Phys. Rev. B **26**, 2790 (1982); A. J. Freeman, H. Krakauer, S. Ohnishi, Ding-Sheng Wang, M. Weinert, and E. Wimmer, J. Phys. (Paris) Colloq. **43**, C7-167 (1982); A. J. Freeman, J. Magn. Magn. Mater. **35**, 31 (1983): H. Krakauer, A. J. Freeman, and E. Wimmer, Phys. Rev. B **28**, 610 (1983).

[3]A. J. Freeman and C. L. Fu, J. Appl. Phys. **61**, 15 (1987).

[4]G. W. Fernando and B. R. Cooper, Phys. Rev. B **38**, 3016 (1988).

[5]J. I. Lee, C. L. Fu, and A. J. Freeman, J. Magn. Magn. Mater. **62**, 93 (1986); C. Li, A. J. Freeman, and C. L. Fu, *ibid.* **75**, 53 (1988).

[6]R. Richter, J. G. Gay, and J. R. Smith, Phys. Rev. Lett. **54**, 2704 (1985); C. L. Fu, A. J. Freeman, and T. Oguchi, *ibid.* **54**, 2700 (1985).

[7]C. Li, A. J. Freeman, and C. L. Fu, J. Magn. Magn. Mater. **75**, 201 (1988).

[8]S. Blugel, M. Weinert, and P. H. Dederichs, Phys. Rev. Lett. **60**, 1077 (1988).

[9]S. Ohnishi, M. Weinert, and A. J. Freeman, Phys. Rev. B **30**, 36 (1984).

[10]C. L. Fu and A. J. Freeman, Phys. Rev. B **35**, 925 (1987).

[11]W. Marshall and S. W. Lovesey, *Theory of Thermal Neutron Scattering* (Oxford University Press, Oxford, England, 1971).

[12]J. Schoenes and W. Reim, J. Magn. Magn. Mater. **54-57**, 1371 (1986).

[13]A. J. Bennet and B. R. Cooper, Phys. Rev. B **3**, 1642 (1971).

[14]H. Takyama, K. Bohnen, and P. Fulde, Phys. Rev. B **14**, 2287 (1976).

[15]J. G. Gay and R. Richter, Phys. Rev. Lett. **56**, 2728 (1986).

[16]C. LI, A. J. Freeman, H. J. F. Jansen, and C. L. Fu, Phys. Rev. B **42**, 5433 (1990).

[17]P. Bruno, Phys. Rev. B **39**, 865 (1989).

[18]M. B. Stearns, Landolt-Börnstein, New Series Vol. III/19a (Berlin, Springer, 1984).

[19]O. Eriksson, G. W. Fernando, R. C. Albers, and A. M. Boring, Solid State Commun. **78**, 801 (1991).

[20]H. Krakauer and B. R. Cooper, Phys. Rev. B **16**, 605 (1977); C. Q. Ma, M. V. Ramana, B. R. Cooper, and H. Krakauer, J. Vac. Sci. Thechnol. A **1**, 1095 (1983); C. Q. Ma, M. V. Ramana, B. R. Cooper, and H. Krakauer, Phys. Rev. B **34**, 3854, (1986); G. W. Fernando, B. R. Cooper, M. V. Ramana, H. Krakauer, and C. Q. Ma, Phys. Rev. Lett. **56**, 2299 (1986).

[21]O. K. Andersen, Phys. Rev. B **12**, 3060 (1975); H. L. Skriver, *The LMTO Method* (Springer, Berlin, 1984).

[22]S. H. Vosko, L. Wilk, and N. Nusair, Can. J. Phys. **58**, 1200 (1980).

[23]M. S. S. Brooks and P. J. Kelly, Phys. Rev. Lett. **51**, 1708 (1983).

[24]H. Kobayashi and S. Kato, Surf. Sci. **12**, 398 (1986); K. Ueda, and R. Shimizu, Jpn. J. Appl. Phys. **12**, 1869 (1973); A. M. Turner, Yu. J. Chang, and J. L. Erskine, Phys. Rev. Lett. **48**, 348 (1982).

[25]D. R. Eastman, Phys. Rev. B **2**, 1 (1970).

[26]W. Eib and S. F. Alvarado, Phys. Rev. Lett. **37**, 444 (1976).

[27]R. W. Strayer, W. Mackie, and L. W. Lawson, Surf. Sci. **34**, 225 (1973); G. G. Tibbetts, J. M. Burkstrand, and J. C. Tracy, Phys. Rev. B **15**, 3652 (1977); G. A. Haas and R. E. Thomas, J. Appl. Phys. **48**, 86 (1987).

[28]V. L. Moruzzi, P. M. Marcus, and J. Kübler, Phys. Rev. B **39**, 6957 (1989); J. Kübler, Phys. Lett. **81A**, 81 (1981).

[29]O. K. Andersen, J. Madsen, U. K. Poulsen, O. Jepsen, and J. Kollar, Physica **86-88B**, 249 (1977).

[30]O. Eriksson, B. Johansson, R. C. Albers, A. M. Boring, and M. S. S. Brooks, Phys. Rev. B **42**, 2707 (1990).

[31]H. Ebert, R. Zeller, B. Drittler, and P. H. Dederichs, J. Appl. Phys. **67**, 4576, (1990).

[32]C. S. Wang, B. M. Klein, and H. Krakauer, Phys. Rev. Lett. **54**, 1852 (1985); F. J. Pinski, J. Staunton, B. L. Gyorffy, D. D. Johnson, and G. M. Stocks, *ibid.* **56**, 2096 (1986); P. Bagno, O. Jepsen, and O. Gunnarsson, Phys. Rev. B **40**, 1997 (1989); D. J. Sing, W. E. Pickett, and H. Krakauer, *ibid.* **43**, 11 628 (1991).

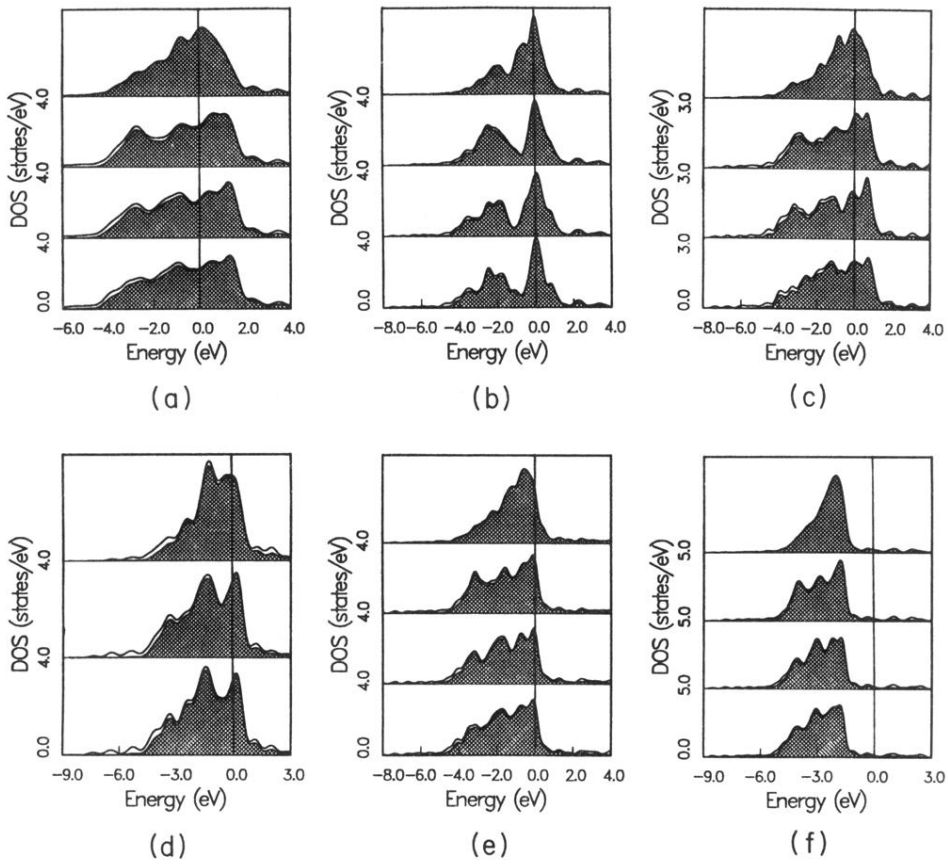

FIG. 1. Paramagnetic density of states (DOS) for fcc Mn (a), bcc Fe (b), fcc Fe (c), hcp Co (d), fcc Ni (e), and fcc Cu (f). The Fermi level is at zero and is marked with a vertical line, and units are in eV. The bulk to surface projected DOS are shown from bottom to top, respectively. The shaded area represents the 3*d* partial DOS.

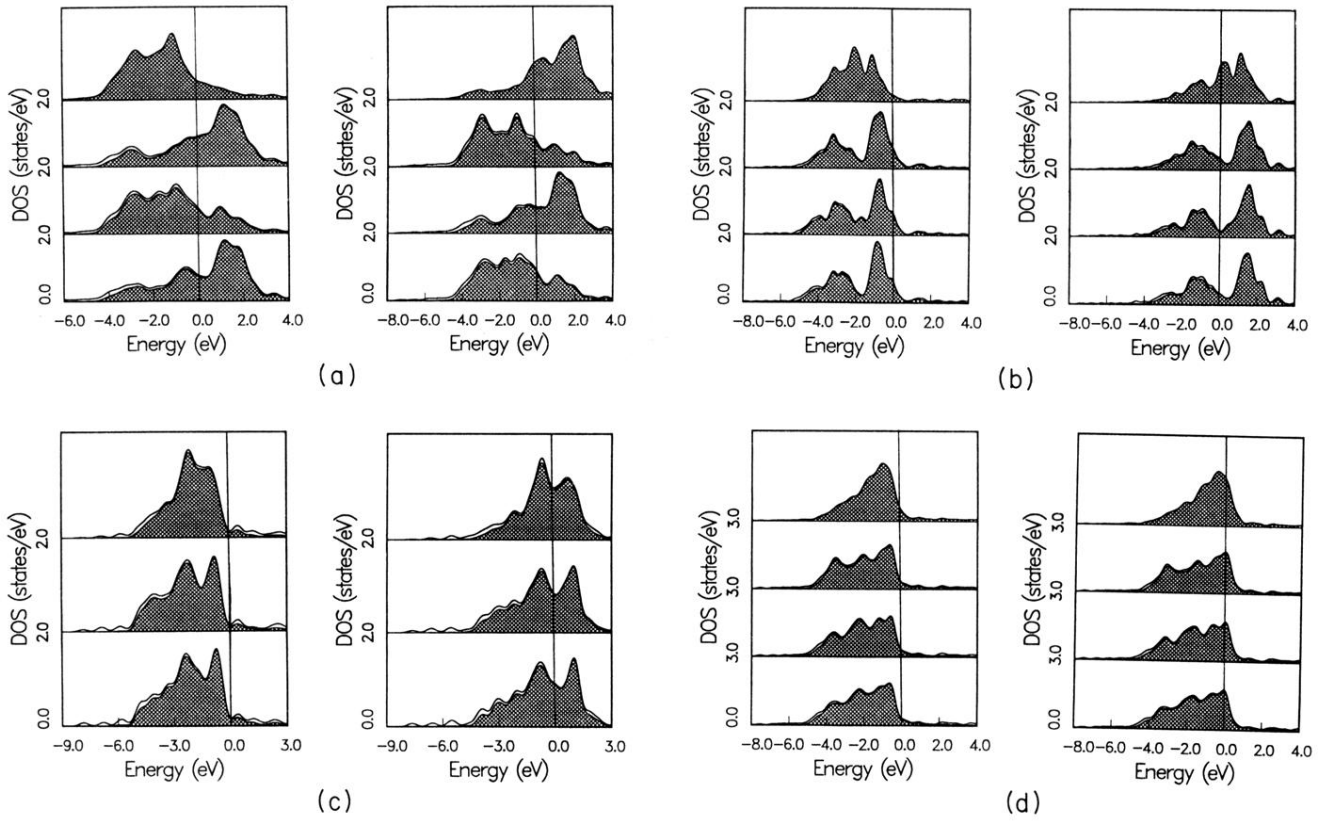

FIG. 3. Spin-polarized density of states (DOS) for fcc Mn (a), bcc Fe (b), hcp Co (c), and fcc Ni (d). The Fermi level is at zero and is marked with a vertical line, and units are in eV. The bulk to surface projected DOS are shown from bottom to top, respectively. The shaded area represents the 3*d* partial DOS. The spin-up DOS is to the left in the figure, and the spin-down DOS is to the right.

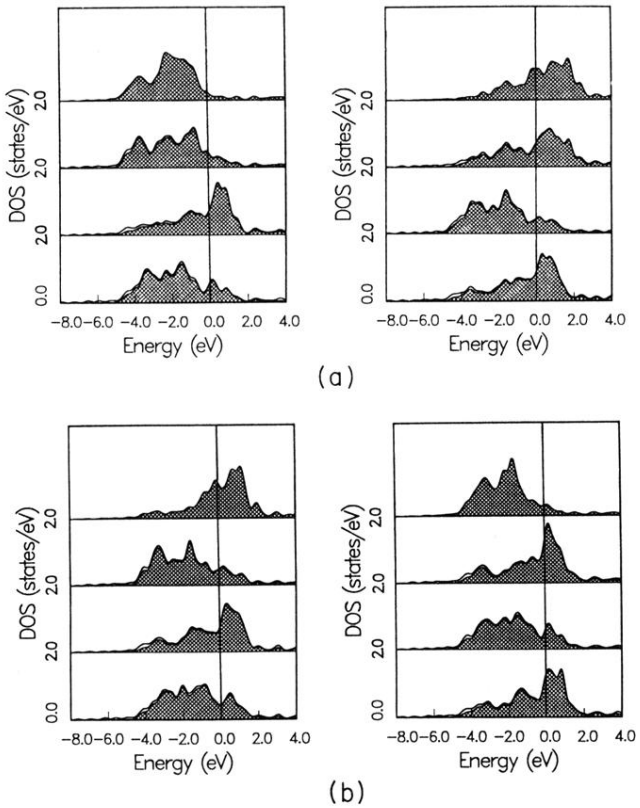

FIG. 4. Spin-polarized density of states (DOS) for the seven-layer calculation of Fe. The $++-+-++$ configuration is shown in (a) and the $-+-+-+-$ configuration is shown in (b). The Fermi level is at zero and is marked with a vertical line, and units are in eV. The bulk to surface projected DOS are shown from bottom to top, respectively. The shaded area represents the 3*d* partial DOS. The spin-up DOS is to the left in the figure, and the spin-down DOS is to the right.